Science of the Total Environment 1011 (2026) 181174

Contents lists available at ScienceDirect

Science of the Total Environment

journal homepage: www.elsevier.com/locate/scitotenv

Comprehensive evaluation of the hydrology, pollutant removal, and carbon sequestration performance of biochar-enriched bioretention soil

Chia-Chun Ho [a,*], Yu-Qian Su [a], Pen-Chi Chiang [b]

[a] Department of Civil and Construction Engineering, National Taiwan University of Science and Technology, Taipei, 106335, Taiwan
[b] Graduate Institute of Environmental Engineering, National Taiwan University, Taipei, 106335, Taiwan

HIGHLIGHTS

- Biochar improves hydrology, water quality, and carbon sequestration in bioretention.
- Biochar increases soil permeability, water retention, and storm resilience.
- 2.5 % biochar yields 94.5 % COD removal, offering cost-effective pollutant control.
- 5 % biochar achieves superior nitrate removal and high carbon sequestration.
- 10 % biochar maximizes carbon sequestration but yields lower nitrate and COD removal.

GRAPHICAL ABSTRACT

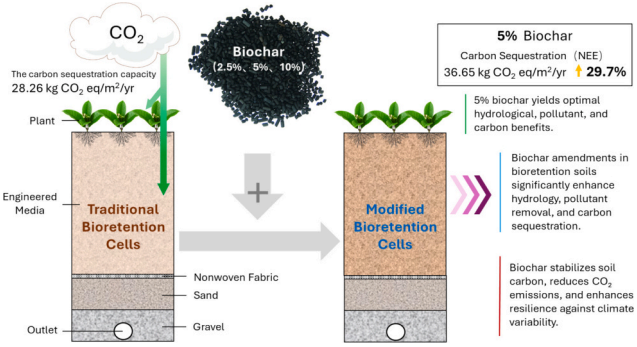

ARTICLE INFO

Keywords:
Low impact development (LID)
Bioretention
Biochar
Carbon sequestration
Soil carbon sequestration
Sustainable development

ABSTRACT

Low impact development (LID) systems effectively reduce stormwater runoff and improve water quality. In addition, their potential contributions to carbon sequestration and climate change adaptation have attracted growing research attention. This study investigated the influence of biochar content on the performance of bioretention cells. A series of experiments was conducted to evaluate eight key indicators: saturated hydraulic conductivity (K_{sat}), water holding capacity, removal efficiencies for ammonium nitrogen (NH_4-N), nitrate nitrogen (NO_3-N), phosphate (PO_4^{3-}-P), and chemical oxygen demand (COD); CO_2 sequestration flux; and soil organic carbon content. The results indicate that biochar amendments significantly improve the functionality of LID systems. Furthermore, the addition of 2.5 % biochar effectively enhances soil hydrological properties, creating favorable conditions for plant growth. The addition of 5 % biochar results in optimal pollutant removal and water purification, thus serving as a well-balanced and efficient treatment strategy. Moreover, the addition of 10 % biochar results in optimal carbon sequestration, demonstrating the role of biochar in strengthening soil carbon sinks. However, excessive biochar content may affect microbial activity and nutrient pathways,

Abbreviations: ANOVA, analysis of variance; CH_4, methane; CO_2, carbon dioxide; COD, chemical oxygen demand; DOC, dissolved organic carbon; FTIR, Fourier transform infrared spectroscopy; GHG, greenhouse gas; GWP, global warming potential; HSD, honestly significant difference (Tukey HSD test); K_{sat}, saturated hydraulic conductivity; LID, low impact development; N_2O, nitrous oxide; NH_3–N, ammonia nitrogen; NO_3^-, nitrate; OC, organic carbon; PBBR, peat-based bioretention with biochar; PBR, peat-based bioretention; PO_4^{3-}, orthophosphate; QP, quality performance; SD, standard deviation; SEM, scanning electron microscopy; SOC, soil organic carbon; WHC, water holding capacity.

* Corresponding author.
E-mail address: cchocv@mail.ntust.edu.tw (C.-C. Ho).

https://doi.org/10.1016/j.scitotenv.2025.181174
Received 2 June 2025; Received in revised form 4 December 2025; Accepted 7 December 2025
Available online 16 December 2025

potentially leading to reductions in NO_3-N and COD removal efficiencies. This study provides practical guidance for optimizing biochar use in LID systems to support stormwater management, water quality improvement, and long-term climate mitigation through soil-based carbon storage.

1. Introduction

Global warming has led to an increase in the frequency and severity of extreme weather events, such as typhoons, heavy rainfall, and heat waves, resulting in human society and national economies facing growing risks and challenges. Consequently, the United Nations introduced the Sustainable Development Goals in 2015, focusing on concepts such as sustainable cities, climate action, and water quality. These goals highlight the importance of integrating climate adaptation, carbon reduction, and pollution control into infrastructure planning. In this context, low impact development (LID) systems have gained widespread adoption because they can be used to manage stormwater runoff, reduce pollutant loads, and support environmental sustainability (Batalini de Macedo et al., 2022).

Bioretention cells, which are also called rain gardens, are among the most widely used LID technologies. They enhance infiltration, decrease peak flow rates, and alleviate the pressure on urban drainage infrastructure, ultimately contributing to flood mitigation and groundwater recharge (Davis, 2008; Kazemi et al., 2011). Moreover, the engineered media in these cells support microbial and plant growth, improving nutrient removal from stormwater (Davis et al., 2009; Roy-Poirier et al., 2010).

Several studies have begun to explore the carbon sequestration potential of LID systems. The vegetation within bioretention cells can capture atmospheric CO_2 through photosynthesis, storing it in biomass and soils (Kim et al., 2013; Li et al., 2018; Li et al., 2017; Mao et al., 2017; Nair et al., 2014). These cells are estimated to realize up to 70 % of their total carbon reduction potential over a 30-year lifespan (Kavehei et al., 2018).

A study conducted in Sichuan Province (Fan et al., 2020), China incorporated waste-derived materials into LID systems and quantified the carbon sequestration effects of these systems by examining changes in soil organic carbon (SOC) and plant biomass contents. The systems exhibited carbon storage rates of 6.47–12.8 kg C/m^2/year, which corresponds to 23.72–46.93 kg CO_2 eq/m^2/year after applying standard conversion factors. Additionally, LID systems in Iran were evaluated by measuring vegetation-based carbon sequestration and reductions in operational energy use (Seyedabadi et al., 2021). The systems exhibited annual sequestration rates of 6.99–9.29 kg C/m^2year, equivalent to 25.66–34.06 kg CO_2 eq/m^2/year. Furthermore, elemental analyzers were used to measure soil carbon content in 25 LID systems across Australia (Kavehei et al., 2019). The average sequestration rate of these systems was 0.31 kg C/m^2/year, which is equivalent to approximately 1.14 kg CO_2 eq/m^2/year. Another study examined LID systems in Argentina, estimating carbon sequestration for a single growing season by accounting for plant biomass (both above and below the ground) and SOC (Robbiati et al., 2023). The maximum seasonal carbon storage was 2.74 kg CO_2 eq/m^2. When the energy savings associated with LID operations were factored in, the annual reduction in carbon emissions reached 70.83 kg CO_2 eq/m^2/year.

However, the carbon sequestration potential of such systems remains inconsistently reported because of differing regional conditions, measurement approaches, and conversion assumptions. Furthermore, no standardized framework exists for comparing carbon sequestration outcomes across studies, particularly when amendments are added to bioretention media.

Studies have employed soil amendments such as biomass and biochar to improve the cell functionality and carbon sequestration performance of bioretention media. Biomass (derived from organic matter) offers benefits such as sustainability and enhanced plant growth, which indirectly promote CO_2 uptake and contributes to long-term carbon sequestration (Oldfield et al., 2018; Quan et al., 2023; Sanchez-Monedero et al., 2018; Vassilev et al., 2010). Compost, a common biomass derivative, enhances soil fertility, infiltration, and water retention while also stabilizing soil structure and improving nutrient uptake efficiency (Celik et al., 2010; Mensah and Frimpong, 2018; Rivers et al., 2021; Sayara et al., 2020).

Biochar, which is produced through the pyrolysis of biomass under oxygen-limited conditions, is a stable, carbon-rich material with high porosity and a large surface area. This material improves soil permeability and water retention while directly enhancing carbon storage through physical adsorption and chemical interactions (Deng et al., 2014; Serafin et al., 2017; Singh et al., 2022). Studies have confirmed the strong CO_2 adsorption potential of biochar and its ability to increase SOC and aggregation stability (Ji et al., 2022; Liu et al., 2022; Wu et al., 2023). However, its effects vary with the type of biochar, pyrolysis temperature, particle size, and application rate (He et al., 2017; Ji et al., 2018). In addition to enhancing carbon storage, biochar can remove pollutants from runoff and reduce nutrient leaching, supporting water quality improvements (Li et al., 2017). However, its performance is influenced by environmental and application-specific factors, which must be carefully considered to ensure it is optimally used (Günal et al., 2018; Li et al., 2021).

Despite the demonstrated benefits of LID systems, most carbon-related studies have focused only on construction-stage emissions or vegetation growth; and consequently have overlooked the synergistic effect of engineered media composition and soil amendments on carbon sequestration. Furthermore, few studies have comprehensively evaluated the combined effect of water regulation, pollutant removal, and carbon capture. To address these gaps, the present study conducted a series of laboratory-scale experiments to quantify the carbon sequestration potential of bioretention cells and evaluate their hydrological and water quality performance. This study had two objectives: (1) to assess the hydrological regulation, pollutant removal, and carbon sequestration performance of biochar-amended bioretention soils and (2) to determine which amendment levels provided the most balanced overall benefits. These study hypothesized that a moderate addition of biochar would result in the optimal trade-off by simultaneously enhancing infiltration capacity, nutrient removal efficiency, SOC stabilization, and carbon sequestration potential and avoiding the negative trade-offs associated with either insufficient or excessive application rates. The findings of this study can support the development of multifunctional, low-carbon LID strategies that contribute to net-zero goals, climate resilience, and sustainable urban development.

2. Materials and methods

This study conducted a series of laboratory-scale experiments to identify the optimal composition of engineered bioretention media for enhancing carbon sequestration. The hydrological, water quality, and carbon sequestration performance of bioretention cells with different compositions were comprehensively evaluated. The experimental process consisted of two main phases. Phase I involved the evaluation of the carbon sequestration potential of four types of biomass, each of which was incorporated at a consistent percentage into engineered bioretention media. The goal of this phase was to assess the contribution of each type of biomass to soil carbon storage. In Phase II, the best-performing biomass from Phase I was used to create new bioretention cells with varying biochar contents. Subsequently, the hydrological, pollutant removal, and carbon sequestration performance of these cells

was assessed to determine the optimal biochar content.

2.1. Experimental design

Each bioretention column was constructed using a polyvinyl chloride pipe with a height of 100 cm and a diameter of 20 cm. The bottom of the pipe was filled with 10 cm of gravel, following which 10 cm of coarse sand, 60 cm of engineered media, and a surface layer of gravel mulch were added in sequence. Vegetation was then planted on the surface layer (Fig. 1). This configuration was used for both the Phase I and the Phase II experimental samples, with the configuration differing only in terms of the composition and amendment ratio of the engineered media. *Osmanthus fragrans*, a commonly used evergreen shrub in Taiwanese bioretention cells, was selected as the vegetation species because of its adaptability to humid and well-drained subtropical environmental conditions.

To ensure adequate infiltration, the base engineered media consisted of 70 % native soil, 10 % perlite, 10 % vermiculite, and 10 % peat, which also ensured sufficient fertility for plant growth. This composition served as the control medium (i.e., a peat bioretention [PBR] medium). In the Phase I experiments, the 10 % peat from the control PBR medium was replaced with 10 % organic compost, 10 % biochar, and a mixture of 3 % compost and 7 % biochar to produce compost bioretention (CBR), biochar bioretention (BBR), and biocompost bioretention (BCBR) media, respectively.

In the Phase II experiments, the effects of biochar proportion on the overall performance of the constructed bioretention cells were assessed. Biochar was added to the control PBR medium to obtain PBR media with 2.5 %, 5 %, and 10 % of biochar by volume, with these designated as PBBR2.5 %, PBBR5%, and PBBR10%, respectively. In these treatments, the biochar was added over the original PBR medium rather than as a substitute for any component. In the Phase II experiments, the effects of biochar proportion on the overall performance of the constructed bioretention cells were assessed. Biochar was added to the control PBR medium to obtain PBR media with 2.5 %, 5 %, and 10 % of biochar by volume, with these designated as PBBR2.5 %, PBBR5%, and PBBR10%, respectively. In these treatments, the biochar was added over the original PBR medium rather than as a substitute for any component.

The selection of amendment levels was guided by relevant literature and practical considerations. Related studies have commonly added 2 %–10 % biochar by volume to bioretention or LID systems. Their findings have indicated that the addition of <2 % biochar by volume results in negligible improvements (including hydraulic properties and carbon sequestration capacity), whereas the addition of >10 % biochar can lead to alteration of the pore structure, a decrease in hydraulic conductivity, and a release of excessive dissolved organic carbon (Akpinar et al., 2023; Goldschmidt and Buffam, 2023; Sheng and Zhu, 2018). To capture the effects of biochar concentration on the constructed bioretention media, this study selected biochar concentrations of 2.5 % and 5 % to represent cost-effective but effective treatments. Moreover, it selected a biochar concentration of 10 % to represent high-end treatment to assess the upper limit of potential performance gains when the material cost is low. The hydrological regulation, pollutant removal, and carbon sequestration performance across these biochar concentrations was comprehensively compared to identify the optimal biochar volume percentage.

The native soil used in this study was a slightly acidic sandy silty soil (USCS classification: SM), which is representative of common bioretention media in northern Taiwan. Peat was derived from decomposed coconut coir. Commercially available horticultural organic compost produced in Taiwan was used in this study. This compost consisted of a matured mixture of wood chips, rice husks, fruit and vegetable residues, and a small proportion of poultry manure. The compost was processed through high-temperature aerobic fermentation to ensure pathogen inactivation and seed sterilization. The biochar used in this study was derived from renewable bamboo resources cultivated in central and southern Taiwan (Fig. 2). It was produced through low-temperature pyrolysis at approximately 300 °C under oxygen-limited conditions and then ground and sieved to a particle size of 0.85–2 mm. Bamboo was selected as the feedstock for biochar preparation because of its abundance, rapid growth, and year-round harvestability in subtropical regions. To control for particle size effects, the biochar, peat, and compost were sieved to comparable particle sizes, namely 0.85–2 mm (between

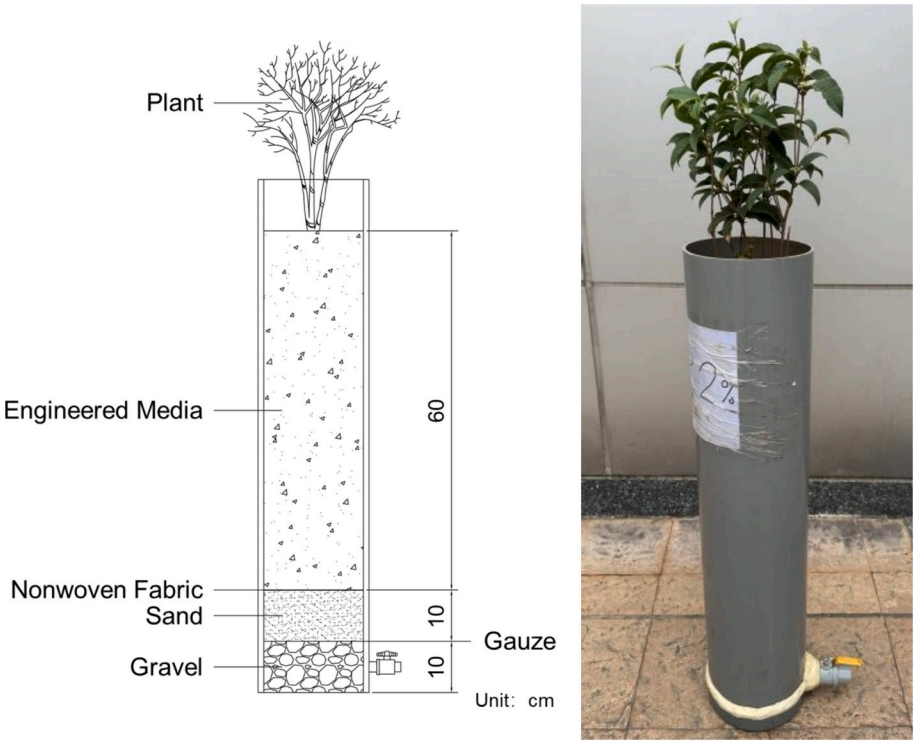

Fig. 1. Schematic and photograph of a bioretention cell constructed in this study.

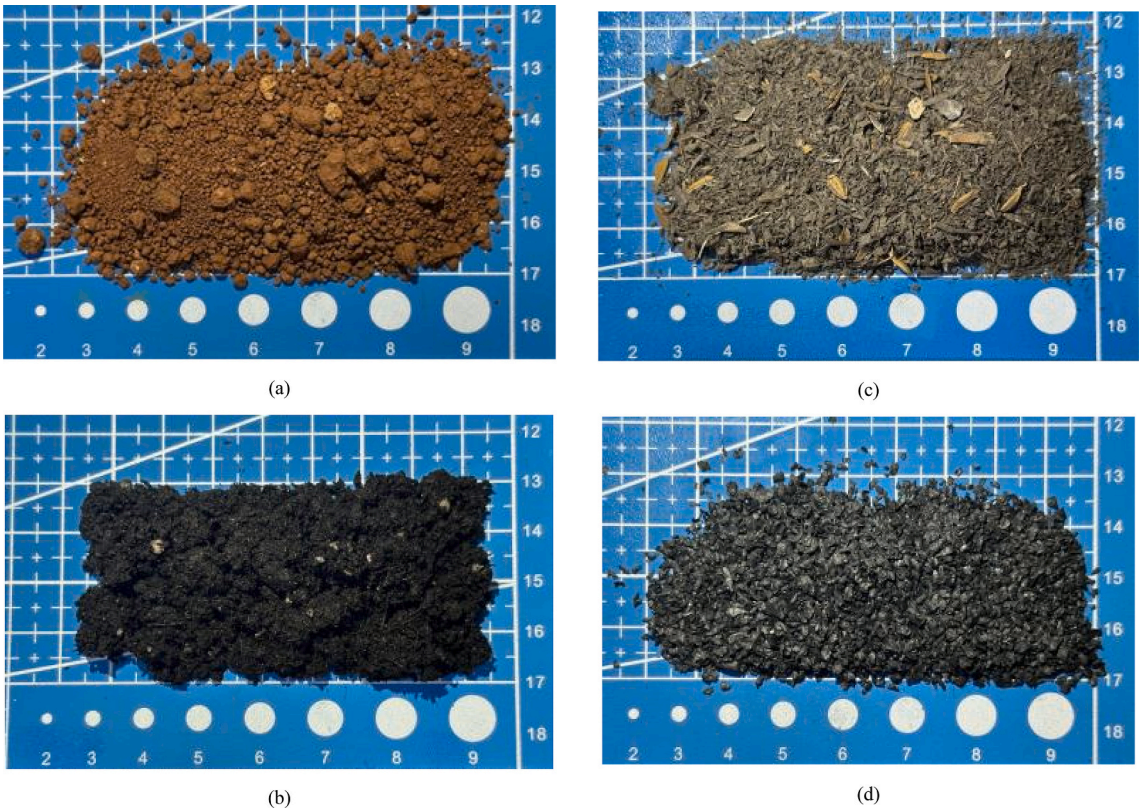

Fig. 2. Test materials: (a) native soil, (b) peat, (c) compost, and (d) biochar.

the #10 and #20 sieve), 0.5–2 mm (between the #20 and #35 sieve), and 0.2–2.5 mm (between the #8 and #70 sieve) respectively (Alghamdi et al., 2020; de Jesus Duarte et al., 2019).

2.2. Measurements

The experiments in this study involved three steps: hydrological measurement, water quality measurement, and carbon adsorption measurement. Table 1 summarizes the experimental process, which is explained in detail in the following text.

2.2.1. Hydrological measurement

Bioretention cells are well known for their ability to reduce stormwater runoff during intense rainfall events. Their performance in doing so substantially depends on two key soil properties, namely, saturated hydraulic conductivity (K_{sat}) and water holding capacity (WHC). This study, conducted controlled experiments to explore whether the type of biomass in engineered bioretention media influences these hydrological properties and thus affects the stormwater mitigation performance of bioretention media.

The K_{sat} values of the constructed bioretention media were determined using the constant head test in accordance with the ASTM D2434-68 (2006) standard. During this test, the outlet valve at the base of the tested bioretention column was closed, and the entire column was filled with water and left undisturbed for over 24 h to ensure saturation of the engineered media. Subsequently, the outlet valve was opened, and

Table 1
Summary of the experimental process.

Experimental groups		Phase I experiment	Phase II experiment
Scenario setting		• 10 % peat bioretention (PBR) • 10 % compost bioretention (CBR) • 10 % biochar bioretention (BBR) • 3 % compost and 7 % biochar bioretention (BCBR)	• 10 % peat bioretention (PBR) • Peat-based bioretention with 2.5 % biochar (PBBR2.5 %) • Peat-based bioretention with 5 % biochar (PBBR5%) • Peat-based bioretention with 10 % biochar (PBBR10%)
Hydrological measurement	saturated hydraulic conductivity (K_{sat})	✓ (The experiment lasted a total of 6 months)	✓ (The experiment lasted a total of 12 months)
	Water holding capacity (WHC)	X	✓
Water quality measurement	Orthophosphate (PO_4^{3-}) Nitrate nitrogen (NO_3-N) Ammonia nitrogen (NH_4-N) Chemical oxygen demand (COD)	X	✓ (The experiment lasted a total of 12 months)
Carbon adsorption measurement	Closed chamber method (CO_2 flux)	✓ (The experiment lasted a total of 6 months)	✓ (The experiment lasted a total of 12 months)
	Walkley-Black method (soil organic carbon)	✓ (Measurements were conducted before and after the closed-chamber experiment, spanning a total period of six months)	✓ (Measured every two months, for a total duration of 12 months)

water was continuously supplied at the top to maintain a constant water level. This step enabled the removal of trapped air from the pore spaces in the engineering media (Jačka et al., 2018). After the outflow rate stabilized, the discharge volume (Q) was recorded, and K_{sat} was calculated using Darcy's law as follows:

$$K_{sat} = \frac{Q \bullet L}{\Delta h \bullet A \bullet t} \quad (1)$$

where:

K_{sat} = saturated hydraulic conductivity (cm/s),
Q = discharge volume (cm^3),
L = thickness of the engineered media (cm),
A = cross-sectional area of the column (cm^2),
Δh = hydraulic head difference between the inflow and the outflow (cm),
t = duration of the outflow (s).

WHC was assessed immediately following the constant head test. After water injection was stopped, the drainage valve remained open, and the column was left to drain until no further outflow occurred. At this point, soil samples were collected from the engineering media to determine their saturated masses. The samples were then dried in an oven at 105 °C for 24 h to enable determination of their dry mass. Subsequently, WHC values were calculated as the difference between the saturated and dry soil masses (Jačka et al., 2018; Kinney et al., 2012) by using the following equation:

$$WHC(\%) = \frac{m_1 - m_2}{m_2} \quad (2)$$

where:

m_1 = saturated soil mass (g),
m_2 = dry soil mass after oven drying (g).

2.2.2. Water quality measurement

In addition to runoff volume control, pollutant removal is a key function of bioretention cells. To assess the effect of the composition of engineered media on their pollutant removal performance, this study conducted wastewater treatment tests. Synthetic wastewater was used in these tests, and the types, concentrations, and preparation methods of pollutants were selected with reference to previous research characterizing surface runoff and typical influent conditions for bioretention cells in urban environments (He et al., 2022; Kratky et al., 2021). The composition of the synthetic wastewater used in this study is presented in Table 2.

As illustrated in Fig. 3, the synthetic wastewater was first poured into a storage tank, and then pumped into a water supply tank by using a submersible water pump. A water level controller was employed to maintain a constant water level in the supply tank, which ensured a consistent hydraulic loading rate (HLR) during the experiment. When the supply valve was opened, the wastewater was distributed evenly over the bioretention media through a trickling pipe. After the outflow stabilized, effluent samples were collected from the base of the column and analyzed for water quality.

Table 2
Composition of the synthetic wastewater used in this study.

Component	Configure concentration (mg/L)	Medicines used
Orthophosphate (PO_4^{3-})	0.5	KH_2PO_4
Nitrate nitrogen (NO_3-N)	1.0	KNO_3
Ammonia nitrogen (NH_4-N)	2.0	NH_4Cl
Chemical oxygen demand (COD)	40	$C_6H_{12}O_6$ (Glucose)

Water quality testing was conducted in accordance with standardized procedures established by Taiwan's National Institute of Environmental Analysis. These tests were used to evaluate the efficiencies of bioretention cells with different compositions of engineered media in removing nutrients and organic pollutants from effluent.

2.2.3. Measurement of carbon adsorption

Net ecosystem exchange (NEE) represents the net rate of CO_2 exchange between an ecosystem and the atmosphere. It accounts for CO_2 uptake through photosynthetic carbon fixation (carbon sink); CO_2 release from plants through autotrophic respiration (carbon source); and CO_2 release from soil, plant roots, and biochar-associated processes through heterotrophic respiration by microorganisms (carbon source). A positive NEE value indicates net CO_2 release to the atmosphere (net carbon source), whereas a negative NEE value suggests net CO_2 uptake from the atmosphere (net carbon sink). In this study, the flux values measured in a closed-chamber system represent the NEE (Oertel et al., 2016; Xu et al., 2020) because they reflect the overall carbon dynamics of plants, soils, and biochar under prevailing environmental conditions. The chamber contained a transparent acrylic cylinder with an inner diameter of 20 cm, a hight of 50 cm, and a wall thickness of 1 cm. This cylinder was sealed with a transparent acrylic lid equipped with two gas valves for CO_2 injection and exhaust as well as a waterproof cable gland for CO_2 sensor installation (see Fig. 4). To ensure uniform gas mixing and improve CO_2 measurement stability, a small circulation fan was installed inside the chamber. CO_2 gas was injected as required, and the real-time CO_2 concentration was continuously monitored. The CO_2 equivalent flux per unit time was calculated using the ideal gas law as follows:

$$F = \frac{M}{A} \bullet \frac{PV}{RT} \bullet \frac{dc}{dt} \quad (3)$$

where:

F = CO_2 equivalent flux (mg $CO_2/m^2/h$)
M = molar mass of CO_2 (44 g/mol)
P = air pressure inside the chamber (1013.25 hPa)
T = air temperature in the chamber (K)
V = chamber volume (0.0157 m^3)
A = cross-sectional area of the chamber (0.0315 m^2)
dc/dt = change in the CO_2 concentration over time (ppm/h)
R = ideal gas constant (83.145 L·hPa/K·mol)

In addition to NEE, SOC stock was measured to assess carbon sequestration. The Walkley–Black method (dichromate oxidation), a widely used and rapid technique, was employed to determine the soil carbon content (Shamrikova et al., 2022). The obtained carbon concentration (C) was then substituted into Eq. (4) to estimate soil carbon storage (C_{soil}), which was subsequently converted into equivalent CO_2 sequestration (C_{SOC}) as follows by using a standard factor of 3.66 (Gogoi et al., 2021; Granata et al., 2020):

$$C_{SC} = 3.66 \times C_{soil} = 3.66 \times BD \times C \times d \times (1 - G) \times 10 \quad (4)$$

where:

C_{SOC} = soil carbon sequestration (kg CO_2 eq/m^2),
C_{soil} = SOC stock (kg C/m^2),
BD = soil bulk density (g/cm^3),
C = SOC content (%),
d = sampling depth (cm),
G = gravel content (volume fraction of particles with a diameter of >2 mm).

CO_2 concentrations were measured hourly, and the rate of change in this concentration (ppm/h) was substituted into Eq. (3) to calculate

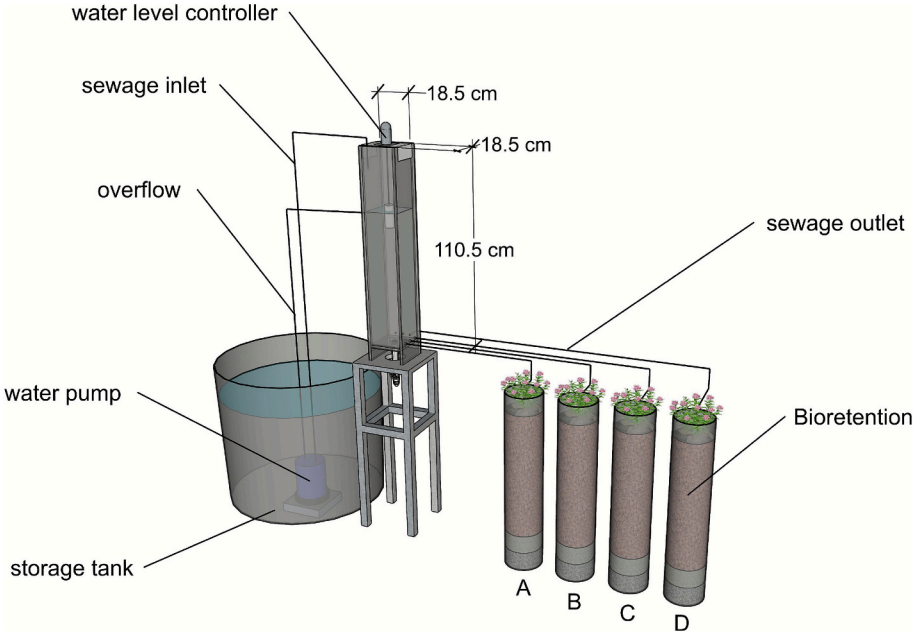

Fig. 3. Schematic of the experimental setup for analyzing the pollutant reduction performance of bioretention cells.

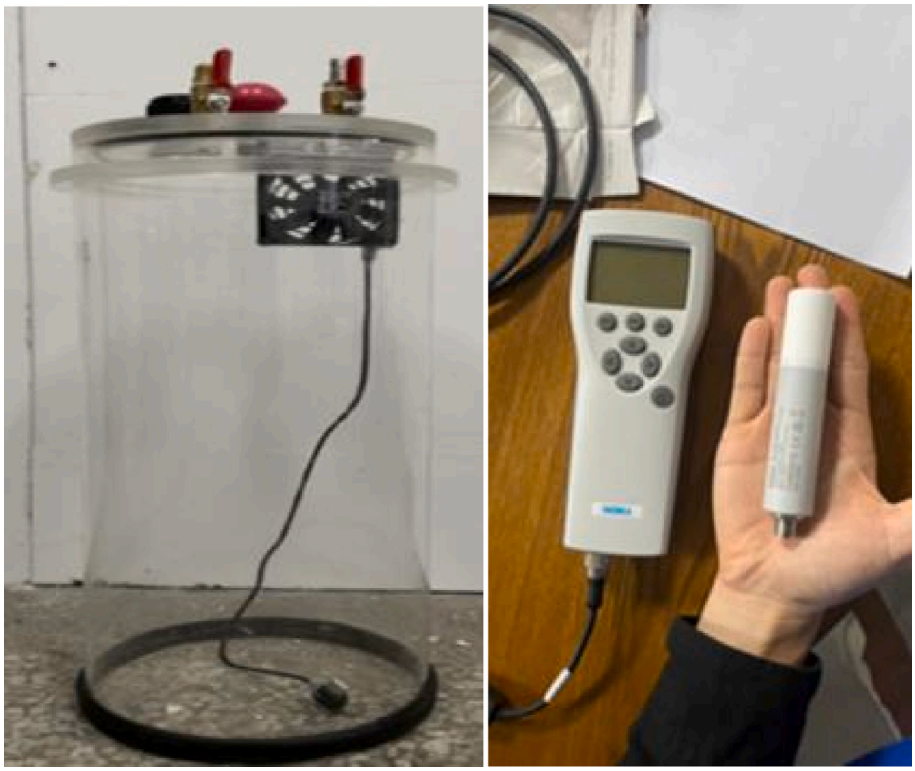

Fig. 4. Closed chamber and CO_2 sensor.

hourly CO_2 flux. Summing hourly values over a 24-h period yielded the daily CO_2 flux, which represents the daily NEE. Soil samples were collected periodically at depths of 5–10 cm from the surface of the bioretention media. The organic carbon content of each sample was converted into soil carbon sequestration (kg CO_2 eq/m^2) by using Eq. (4).

Carbon sequestration was quantified on the basis of the NEE, measured through infrared analysis of the gas in the chamber and periodic SOC sampling. The measured values in this study represent the net CO_2 balance within the experimental bioretention mesocosms for processes occurring inside the bioretention units but excluding those from the raw material supply and construction phases. The results of NEE and SOC for each bioretention cell are expressed on a per-unit-area basis, providing a relative comparison among bioretention systems with different biochar contents.

3. Results and discussion

3.1. Hydrological measurement results

The Phase I experiments were conducted over 6 months by using four parallel bioretention columns. Hydraulic measurements were obtained monthly, with at least three replicates obtained per measurement. The average K_{sat} values are summarized in Table 3. Because the particle sizes of the peat, compost, biochar, and biocompost used in this study were comparable, only marginal variations in K_{sat} were observed. The BBR samples exhibited the highest average K_{sat} values, likely because of the well-developed pore structure, uniform particle size distribution, high cation exchange capacity (CEC), and negative zeta potential of biochar, which promoted ion adsorption/desorption and facilitated water movement through the engineering media (Lu et al., 2023). Conversely, the CBR samples had the lowest average K_{sat} values, and these values gradually decreased over time. These results might be attributable to the decomposition of organic matter and leaching processes, during which fine particles generated through compost degradation possibly clogged the pores and reduced permeability.

On the basis of the aforementioned findings, biochar was selected for further investigation in the Phase II experiments to assess the effect of the amendment ratio on K_{sat}. This phase was conducted under identical conditions over 1 year, with monthly measurements performed thrice and averaged. As displayed in Fig. 5, biochar addition substantially increased and stabilized the K_{sat} values of the bioretention cells.

The control group without biochar (PBR samples) exhibited an annual average K_{sat} value of 0.0392 ± 0.0077 cm/s. By comparison, the biochar-amended samples exhibited considerably higher K_{sat} values. Specifically, the PBR samples with 2.5 %, 5 %, and 10 % biochar (PBBR2.5 %, PBBR5%, and PBBR10%, respectively), exhibited annual average K_{sat} values of 0.0493 ± 0.0013, 0.0601 ± 0.0025, and 0.0513 ± 0.0016 cm/s, respectively; these values are 25.67 %, 53.26 %, and 30.81 % higher than that of the control group, respectively. Thus, the PBBR5 % samples exhibited the highest K_{sat} value.

The results of a one-way analysis of variance (ANOVA) indicated a highly significant treatment effect [$F(3,8) = 593.3$, $p < 0.001$], and Tukey's honestly significant difference (HSD) post-hoc tests suggested that all pairwise comparisons were significant ($p < 0.05$), with the PBBR5 % outperforming every other group. In addition, a repeated measures ANOVA revealed that the biochar content and month had a significant interaction effect on K_{sat} ($p < 0.001$). Although temporal fluctuations occurred in K_{sat}, the K_{sat} rankings of the different groups remained consistent throughout the year, with the PBBR5 % and PBR samples consistently having the highest and lowest K_{sat} values, respectively.

These results suggest that moderate biochar additions significantly improve infiltration capacity and thus help mitigate urban flood risks, while also stabilizing performance over time. The observed decline in K_{sat} at a biochar volume ratio of 10 % may be attributable to changes in soil microporosity, aggregation behavior, or interactions among surface functional groups (Lim et al., 2016).

In contrast to K_{sat}, the WHC consistently increased with the biochar content. The PBR, PBBR2.5 %, PBBR5%, and PBBR10 % groups exhibited WHCs of 49.5 % ± 2.7 %, 52.7 % ± 1.9 %, 53.1 % ± 2.6 %, and 54.2 % ± 2.2 % respectively. This upward trend can be attributed to the highly porous structure, abundant hydrophilic surface functional groups, high CEC, and negative zeta potential of biochar, which enhance soil moisture retention (Ahmad Bhat et al., 2022; Batista et al., 2018; Bikbulatova et al., 2018; Günal et al., 2018).

These findings indicate that incorporating a moderate quantity of biochar into bioretention engineered media can not only enhance their infiltration capacity but also improve their moisture retention, thereby supporting plant growth and reducing long-term irrigation demands and maintenance costs.

Table 3
Saturated hydraulic conductivities (K_{sat}) in Phase I of this study (unit: cm/s).

	PBR	CBR	BBR	BCBR
1st month	0.0341	0.0329	0.0497	0.0435
2nd month	0.0397	0.0315	0.0448	0.0418
3rd month	0.0304	0.0311	0.0403	0.0398
4th month	0.0336	0.0298	0.0341	0.0377
5th month	0.0291	0.0273	0.0376	0.0324
6th month	0.0313	0.0282	0.0319	0.0346
Average	0.0330	0.0301	0.0397	0.0383

3.2. Water quality measurement results

To investigate the effect of biochar addition on the pollutant removal performance of engineered media, synthetic wastewater was introduced monthly into four bioretention columns over 1 year at a constant HLR of 2000 L/m^2/day. Both influent and effluent samples were collected, and their water quality was analyzed.

As presented in Fig. 6(a), the average influent concentration of ammonium nitrogen (NH_4-N) was 2.07 ± 0.163 mg/L, and its average concentrations in effluents collected from the PBR, PBBR2.5 %, PBBR5%, and PBBR10 % samples were 0.25 ± 0.072, 0.23 ± 0.043, 0.22 ± 0.049, and 0.19 ± 0.041 mg/L, respectively. Thus, the aforementioned samples had average NH_4-N removal efficiencies of 87.92 % ± 2.63 %, 89.03 % ± 1.41 %, 89.46 % ± 1.87 %, and 90.95 % ± 1.42 %. These results indicate that the NH_4-N removal efficiency increased marginally with the biochar content. This trend might be attributable to the negatively charged surface of biochar, which effectively adsorbs positively charged NH_4^+ ions (Steiner et al., 2007). Biochar's high surface area, porosity, abundant functional groups, and high CEC also contributed to the enhancement in the NH_4-N adsorption (Dai et al., 2020).

As displayed in Fig. 6(b), the average influent concentration of nitrate nitrogen (NO_3–N) was 1.123 ± 0.068 mg/L, and its average concentrations in the effluents obtained from the PBR, PBBR2.5 %, PBBR5%, and PBBR10 % samples were 0.418 ± 0.110, 0.371 ± 0.074, 0.274 ± 0.051, and 0.444 ± 0.092 mg/L, respectively. Thus, these samples had NO_3–N removal efficiencies of 63.05 % ± 8.18 %, 67.20 % ± 5.01 %, 75.67 % ± 3.79 %, and 60.65 % ± 6.58 %, respectively. These results suggest that moderate biochar addition can modestly enhance NO_3–N removal, whereas excessive biochar addition inhibits NO_3–N removal. The enhancement in NO_3–N removal at a moderate biochar concentration is likely caused by biochar's microstructure, which supports microbial colonization and biofilm formation, promoting the growth of denitrifying bacteria involved in NO_3^- transformation (Xiong et al., 2022; Zhuang et al., 2022). Furthermore, biochar's water retention capacity contributes to prolonged anaerobic conditions and greater contact between NO_3^- and denitrifying microorganisms, thereby enhancing denitrification efficiency (Tian et al., 2019). However, at high biochar contents, biochar's alkaline nature may increase soil pH, alter microbial community composition, and inhibit certain denitrification pathways, particularly those involving N_2O as an intermediate, thus reducing total NO_3–N removal efficiency. In the present study, the PBBR5 % and PBBR10 % samples exhibited the highest and lowest NO_3-N removal rates, respectively.

Fig. 6(c) displays the removal results for orthophosphate (PO_4^{3-}). The average influent concentration of PO_4^{3-} was 0.516 ± 0.022 mg/L, and its average concentrations in the effluents obtained from the PBR, PBBR2.5 %, PBBR5%, and PBBR10 % samples were 0.088 ± 0.013, 0.080 ± 0.015, 0.085 ± 0.012, and 0.078 ± 0.009 mg/L, respectively. Thus, these samples had PO_4^{3-} removal efficiencies of 82.93 % ± 1.98 %, 84.54 % ± 2.49 %, 83.59 % ± 1.94 %, and 84.79 % ± 1.86 %, respectively. The relatively consistent and high phosphate removal efficiencies across all samples suggests that biochar had minimal influence on PO_4^{3-}removal, likely because phosphate removal is primarily governed by precipitation reactions with metal cations such as Fe, Al, and Ca (Feng et al., 2023; Kang et al., 2023; Li et al., 2020). Unless biochar is

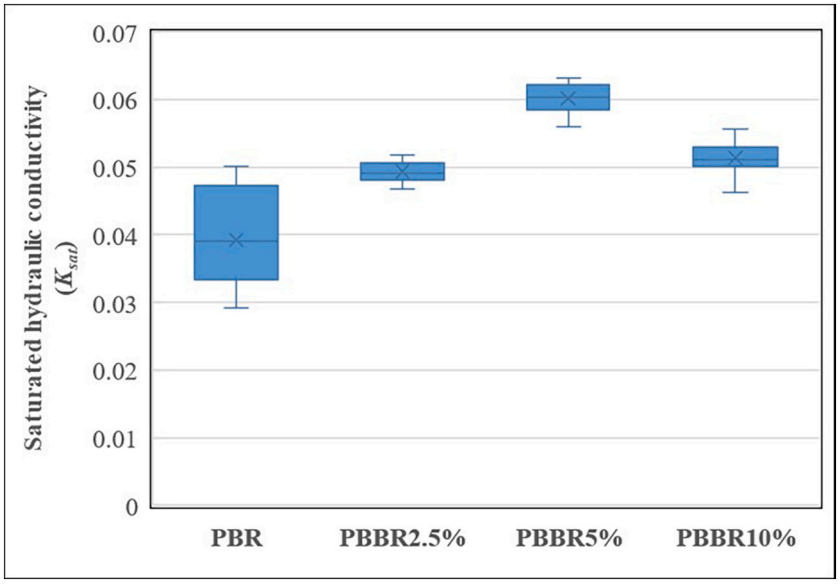

Fig. 5. Saturated hydraulic conductivities (K_{sat}) of different bioretention media in Phase II of thus study.

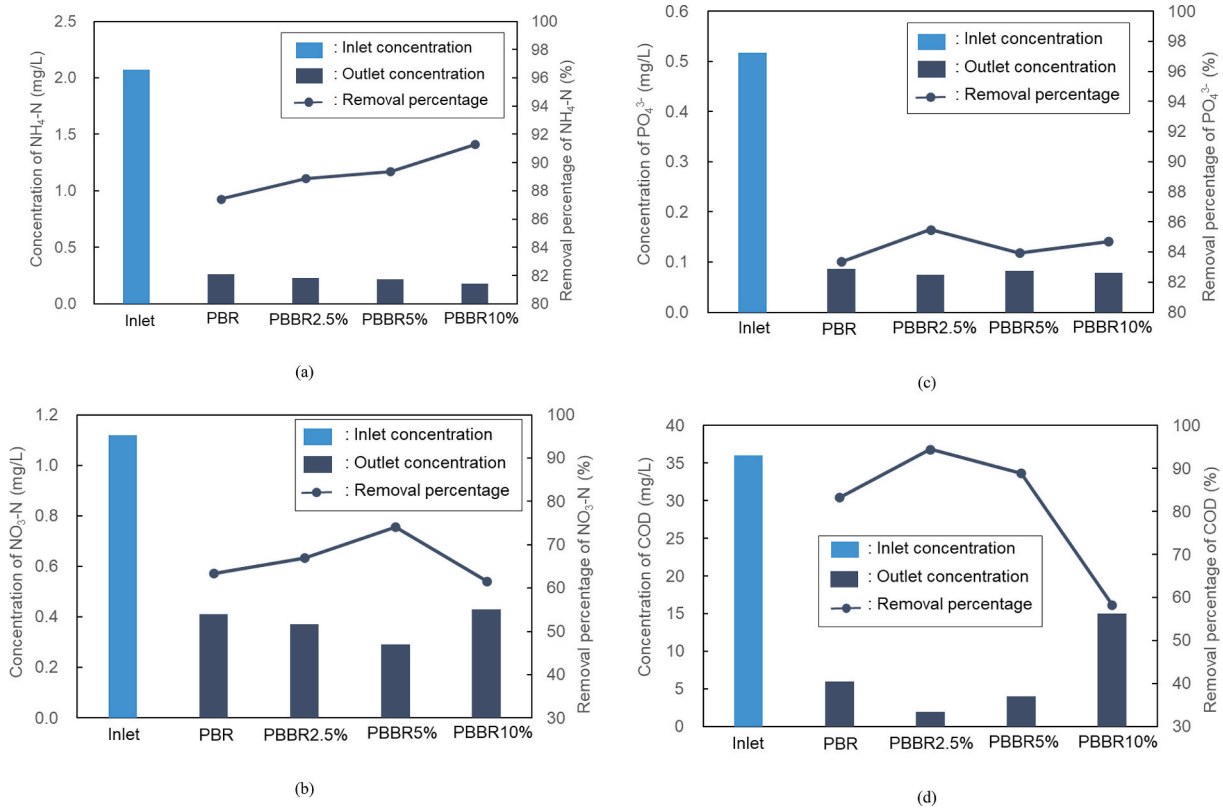

Fig. 6. (a) NH_4-N, (b) NO_3-N, (c) PO_4, and (d) chemical oxygen demand (COD) removal performance of different bioretention columns in Phase II.

enriched with these metal elements, it cannot substantially enhance phosphate removal. In some cases, leaching from phosphorus-rich amendments can even increase PO_4^{3-} concentrations in the effluent (Samaraweera et al., 2023), and consequently, the addition of metal oxides or minerals to biochar may be required to enhance PO_4^{3-} removal (Ulrich et al., 2017).

Fig. 6(d) depicts the chemical oxygen demand (COD) removal performance of the examined samples. The average influent COD was 36.11 ± 1.26 mg/L, and the average COD values of the effluents obtained from the PBR, PBBR2.5 %, PBBR5%, and PBBR10 % samples were 6.03 ± 1.29, 1.99 ± 0.43, 3.98 ± 0.71, and 14.73 ± 1.98 mg/L, respectively. Thus, these samples had COD removal efficiencies of 83.36 % ± 3.08 %, 94.49 % ± 1.12 %, 88.99 % ± 1.73 %, and 59.07 % ± 6.10 %, respectively. The highest COD removal efficiency was exhibited by the PBBR2.5 % samples, whereas the lowest COD removal efficiency was exhibited by the PBBR10 % samples.

COD removal mechanisms in bioretention cells typically involve physical filtration, adsorption, plant uptake, and microbial degradation

(Björklund and Li, 2017). Biochar's high surface area and CEC facilitate organic compound retention when it is added in a moderate quantity. However, fresh biochar may contain residual dissolved organic carbon (DOC) resulting from incomplete pyrolysis. This DOC can leach into the effluent, increasing the COD level (Liu et al., 2019; Mukherjee and Zimmerman, 2013). In this study, the addition of 2.5 % produced minimal DOC leaching and had a limited effect on the COD level. Conversely, the addition of higher biochar contents, especially 10 % by volume, substantially elevated DOC release, reducing net COD removal. Notably, DOC leaching diminished over time. For example, in the early phase of the experiment, the PBBR10 % system achieved a COD removal rate of only 34 %. However, over time, this rate increased to approximately 76 %, suggesting that DOC leaching declined as fresh biochar underwent flushing and microbial stabilization.

To evaluate the statistical differences among the treatments, this study performed a two-way ANOVA with treatment and month as the two factors. Subsequently, Tukey's HSD post-hoc tests were conducted for each pollutant. The results indicate that the treatment effects were significant ($p < 0.05$) for all four pollutants, confirming that biochar addition led to measurable enhancements in removal performance compared with that of the control system.

The effluents obtained from the PBBR10 % samples exhibited the lowest NH_4-N and PO_4^{3-} concentrations (0.188 ± 0.041 and 0.078 ± 0.009 mg/L, respectively), indicating their excellent ammonium and phosphate removal performance. Moreover, the effluents obtained from the PBBR5 % and PBBR2.5 % exhibited the lowest NO_3^- (0.274 ± 0.051 mg/L; mean removal efficiency = 75.67 %) and COD (1.992 ± 0.434 mg/L; mean removal efficiency = 94.49 %) levels, respectively. Overall, the statistical evidence indicates that all biochar treatments resulted in significantly higher removal efficiencies than those exhibited by the control samples. The PBBR5 % samples provided the most balanced overall performance in terms of pollutant removal and hydraulic conductivity, whereas the PBBR2.5 % and PBBR10 % samples offered advantages in removing specific pollutants.

Pollutant removal processes in bioretention systems are not solely governed by adsorption. Microbe-mediated pathways, such as nitrification–denitrification and organic matter degradation, as well as plant uptake may also play crucial roles. However, the present study only focused on evaluating the overall pollutant removal performance of bioretention systems with different biochar contents; it did not employ methods for distinguishing the contributions of individual mechanisms (e.g., microbial community analysis, isotope tracing, or inhibitor-based controls). Therefore, adsorption was considered the primary pollutant removal mechanism in this study. Future research is encouraged to incorporate mechanism-specific analyses to quantify the relative importance of adsorption, microbial processes, and plant uptake to provide a more comprehensive understanding of pollutant removal pathways in biochar-amended bioretention systems.

3.3. Carbon emission results

Fig. 7 displays the NEE measurements obtained in Phase I by using the closed-chamber system. Positive and negative NEE values represent net CO_2 emissions and net CO_2 uptake, respectively. No vegetation was planted before these measurements, and no external CO_2 was injected into the system; thus, changes in CO_2concentration were primarily attributed to soil respiration. The weekly average CO_2 emission rates differed among the four types of bioretention samples examined in Phase I.

The CBR samples exhibited the highest CO_2 emission rate throughout the experiment, with their cumulative CO_2 release over 6 months being 1.452 kg CO_2/m^2, which is substantially higher than those of the other samples. This result can be attributed to the high content of labile organic nitrogen compounds in compost, which undergo microbial mineralization, releasing CO_2, water, and microbial biomass (Sánchez et al., 2015; Tsai and Chang, 2021). Although the CO_2 emission rate of the CBR samples declined over time, it remained consistently higher than those of the other samples.

Compared with the CBR samples, the BBR samples had a lower CO_2 emission rate, with their cumulative CO_2 release over 6 months being of only 0.102 kg CO_2/m^2. This finding underscores the stabilizing effects of biochar in soil systems. The stable molecular structure and strong nutrient retention capacity of biochar enable it to act as a slow-release fertilizer, improve nitrogen use efficiency, and reduce gaseous losses (Yang and Lu, 2021; Zhao et al., 2016). Moreover, biochar enhances nitrogen retention, modulates nitrification and denitrification processes, and reduces CO_2 and N_2O emissions (Irfan et al., 2019; Muñoz et al., 2019; Xu et al., 2014; Yu et al., 2016).

The BCBR samples of this study (3 % compost and 7 % biochar) exhibited an average cumulative CO_2 release of 0.375 kg CO_2/m^2, with their CO_2 release rate being relatively stable throughout the experiment. Thus, the emission rate of the BCBR samples was lower than that of the CBR samples but higher than that of the BBR samples. These results indicate that biochar can mitigate the rapid mineralization associated with compost and stabilize nutrient release over time.

The initial CO_2 emission rate of the PBR samples was higher than those of the BBR and BCBR samples; however, this rate gradually decreased after the 7th week. The cumulative CO_2 release of the PBR samples over 6 months was 0.099 kg CO_2/m^2, indicating that they had the lowest CO_2 emission rate among all samples. This result was likely

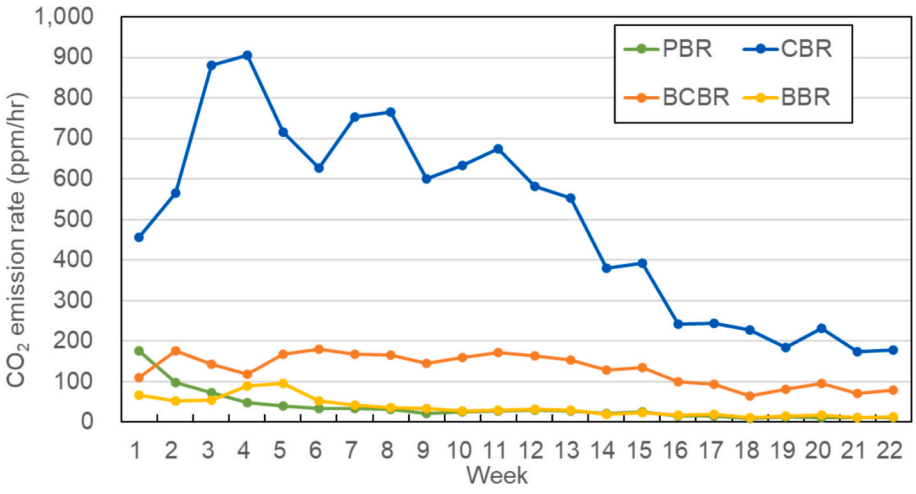

Fig. 7. CO_2 emission results obtained for different types of bioretention samples in Phase I.

caused by the inherently stable nature of peat, which consists of high proportions of organic solids with slow degradation.

In addition to gas flux measurements, SOC content was evaluated before and after the Phase I experiments (6 months) to quantify carbon stock changes. As presented in Table 4, the CBR samples initially exhibited the highest SOC content (1.694 kg C/m^2), followed by the PBR (1.368 kg C/m^2), BCBR (1.043 kg C/m^2), and BBR (0.099 kg C/m^2) samples, respectively. However, by the end of the experiment, the SOC content of the CBR samples dramatically decreased to 0.152 kg C/m^2 (a 91.03 % reduction)., which is consistent with their high mineralization and CO_2 emission rates (Hobbie et al., 2012).

The PBR samples maintained relatively stable SOC levels, exhibiting a decrease of only 2.49 % in SOC during Phase I (from 1.368 to 1.334 kg C/m^2). This result reflects the chemical recalcitrance of peat. The BBR samples exhibited a 60.61 % increase in SOC level (from 0.099 to 0.159 kg C/m^2) during the experiment. This result aligns with the low CO_2 emissions of these samples and highlights the roles played by biochar in promoting microaggregate formation, improving nutrient retention, and reducing organic matter decomposition. These physical and chemical improvements create favorable conditions for microbial activity, reduce carbon loss, and enhance soil productivity and erosion resistance (Yu et al., 2016).

The aforementioned results confirm that although compost considerably enhances soil fertility in the short term, it also induces high CO_2 emissions and rapid organic carbon loss. By contrast, biochar not only stabilizes soil carbon but also improves long-term carbon retention, rendering it a promising material for enhancing the carbon sequestration capability of bioretention cells.

3.4. Carbon sequestration performance of bioretention cells

The results obtained in the Phase I experiments suggest that the addition of an appropriate quantity of biochar to the engineered media in bioretention cells effectively reduces CO_2 emissions and enhances SOC content. Therefore, in the Phase II, the effects of the biochar amendment ratio (2.5 %, 5 %, and 10 %) on the CO_2 sequestration performance of different bioretention systems were evaluated, with both soil and plant-based carbon sinks. *O. fragrans* saplings of similar age and size were planted in each bioretention column for assessment of the contribution of vegetation. NEE was measured using the closed-chamber method, and soil samples were collected every 2 months for regular monitoring of SOC content periodically.

Fig. 8 displays the NEE values obtained for the PBR and PBBR5 % in a 24-h closed-chamber experiment conducted between December 29 and 30, 2024. The closed-chamber experiment commenced at 22:00 on December 29, with plants primarily performing dark respiration in the absence of light and thereby releasing CO_2. The CO_2 concentration at 22:00 was considered the background CO_2 level (F = 0) in calculating the NEE (mg/m^2) per hour per unit area by using Eq. (3), following which the cumulative 24-h NEE (ΣF) was derived. According to the findings of the Phase I experiments, the engineered media contributed to CO_2 emissions through mineralization, which caused an increased in the CO_2 concentration within the sealed chamber. From 08:00 on December 30, the plants began photosynthesis because sunlight became available. Although the plants and soil continued to release CO_2 through respiration, the rate of photosynthetic CO_2 uptake surpassed the total emissions, resulting in a net decrease in NEE. The NEE eventually became negative, indicating net CO_2 uptake by the bioretention system. The CO_2 emissions during the dark respiration phase were notably lower for the PBBR5 % samples than for the PBR samples, suggesting that in addition to plant respiration, biochar effectively suppressed CO_2 emissions produced through soil mineralization. During the photosynthetic phase, the combined effects of CO_2 uptake by the plant and suppressed soil emissions lead to the PBBR5 % samples having substantially lower cumulative NEE values compared with the PBR samples. After 24 h, the total NEE values of the PBR and PBBR5 % samples were 62.20 and 670.52 mg/m^2 (net uptake), respectively, indicating that biochar addition substantially enhanced the CO_2 sequestration capacity of the bioretention system.

Table 4
SOC contents of different samples before and after Phase I.

	Soil organic carbon content (kg C/m^2)			Change rate (%)
	Before	After	Changes	
PBR	1.368	1.334	−0.034	−2.49 %
CBR	1.694	0.152	−1.542	−91.03 %
BBR	0.099	0.159	+0.060	+60.61 %
BCBR	1.043	0.586	−0.457	−43.82 %

A closed-chamber experiment was conducted 1 day per week, and 4 days of experimental data can be obtained per month. The average CO_2 sequestration fluxes of the 4 days were extrapolated to estimate the monthly CO_2 sequestration flux. Over a 1-year period, the monthly average CO_2 sequestration fluxes of the PBR, PBBR2.5 %, PBBR5%, and PBBR10 % were 2.36 ± 0.45, 2.51 ± 0.51, 3.05 ± 0.59, and 3.02 ± 0.64 kg CO_2 eq/m^2, respectively. These results indicate that carbon sequestration flux increased with biochar addition, with the PBBR5 % and PBBR10 % samples exhibiting considerably higher carbon sequestration fluxes than the PBR samples did. Tukey's HSD post-hoc tests indicated that the carbon sequestration flux of the PBR samples was significantly different from those of the PBBR5 % ($p = 0.017$) and PBBR10 % ($p = 0.026$) samples; however, the carbon sequestration fluxes of the PBBR2.5 %, PBBR5%, and PBBR10 % samples exhibited no significant differences. Overall, the aforementioned results indicate that the addition of 5 % biochar resulted in the highest mean carbon sequestration flux, indicating that 5 % is the optimal biochar content and represents the most effective dosage for enhancing long-term carbon sequestration capacity.

As presented in Fig. 9, the monthly CO_2 sequestration flux of each sample group exhibited a clear seasonal trend between February 2024 and January 2025. For all sample groups, this flux gradually increased in the spring, peaked during summer, and decreased during autumn and winter. The highest CO_2 sequestration rates occurred in summer (June and July), indicating elevated carbon uptake during this time. However, extreme weather event, such as persistent high temperatures or continuous rainfall (August and September) temporarily reduced these rates.

The obtained carbon sequestration fluxes suggest that under evenly distributed precipitation and the absence of drought, the *O. fragrans* saplings efficiently used water to conduct CO_2 fixation. Conversely, heavy or prolonged rainfall caused soil saturation, decreased oxygen availability, suppressed root and microbial activity, and ultimately slowed down carbon sequestration. Moreover, high humidity and low light intensity during storms (e.g., typhoons) inhibited photosynthesis, thus affecting carbon uptake. Such conditions may explain the abnormally low fluxes or stagnant flux growth during specific months in the present study. The winter months (December and January) contributed the smallest increases in cumulative flux, with cumulative flux curves approaching a plateau, reflecting the restricted plant growth and microbial activity during this period.

The PBBR2.5 %, PBBR5%, and PBBR10 % samples consistently outperformed the PBR samples in terms of CO_2 sequestration. During the 1-year monitoring period, the cumulative carbon sequestration fluxes of the PBR, PBBR2.5 %, PBBR5%, and PBBR10 % samples were 28.26, 30.06, 36.65, and 36.22 kg CO_2 eq/m^2, respectively. Thus, the carbon sequestration fluxes of the PBBR2.5 %, PBBR5%, and PBBR10 % samples were 6.37 %, 29.68 %, and 28.15 % higher, respectively, than that of the PBR samples. The carbon sequestration flux first increased with the biochar content, peaking at a biochar content of 5 %, and then marginally decreased with a further increase in this content. These findings indicate that moderate biochar addition results in the optimal carbon sequestration effect.

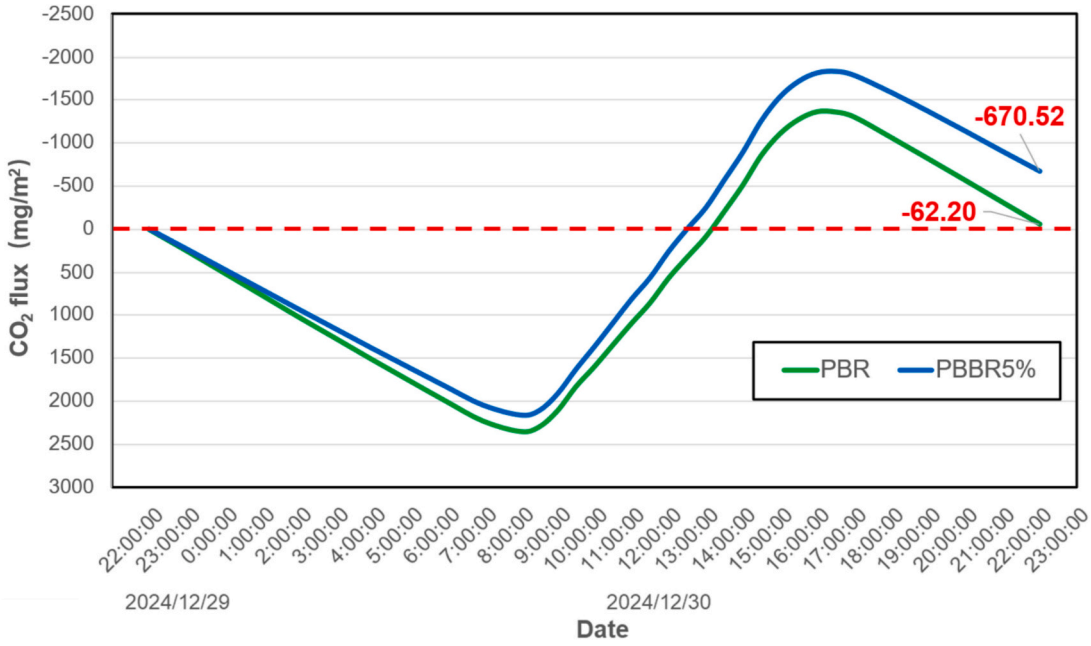

Fig. 8. Hourly NEE values of PBR and PBBR5 % samples during a 24-h closed-chamber experiment.

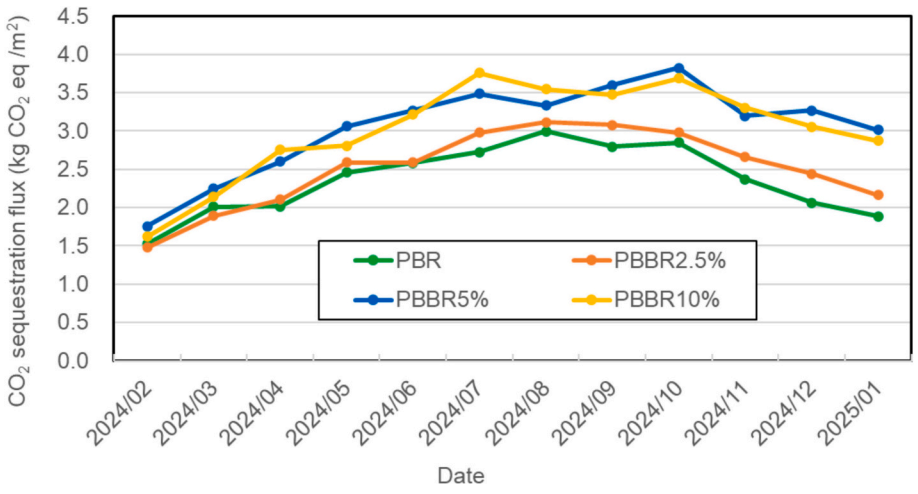

Fig. 9. Variations in the CO_2 sequestration fluxes of different bioretention system over time.

The results of this study are generally consistent with those of previous research on carbon sequestration in bioretention systems (Table 5); however, considerable variations exist across studies. For example, Kavehei et al. (2019) reported a relatively low carbon sequestration rate of 1.14 kg CO_2 eq/m^2/yr, likely because of the arid climate of their Australian study site, poor initial plant establishment, and a failure to consider the sequestration effects of vegetation (only the sequestration effect of soil was considered). By contrast, Robbiati et al. (2023) recorded a sequestration rate of 70.83 kg CO_2 eq/m^2/yr, which was largely attributable to abundant rainfall, rapid vegetation growth, and the consideration of the sequestration effects of aboveground biomass and energy-consumption-related emission reductions. Studies conducted in China and Iran (Fan et al., 2020; Seyedabadi et al., 2021) obtained intermediate carbon sequestration values of 23.72–46.93 and 25.66–34.06 kg CO_2 eq/m^2/yr, respectively. These studies were conducted in semiarid to temperate climates, and they considered both soil and plant sequestration processes, which led to them obtaining values comparable to those of the present study.

The aforementioned discussion highlights that carbon sequestration performance is affected not by a single factor but by multiple interacting variables. For example, climatic conditions and rainfall distribution influence vegetation growth rates and organic matter inputs, and soil physicochemical properties, such as baseline organic carbon and clay fraction, determine carbon stabilization potential. Moreover, plant species and vegetation density affect photosynthetic uptake and litter contributions. Finally, research conditions, such as the presence or absence of aboveground and underground biomass and indirect mitigation effects, substantially influence carbon sequestration results. The absence of standardized measurement conditions and methods explains the wide variations (one order of magnitude) in the carbon sequestration estimates across relevant studies.

Seasonal carbon sequestration performance also varied slightly among the sample groups. For example, during the vegetation's growing season in summer, the PBBR10 % samples exhibited the fastest increase in cumulative carbon sequestration flux, likely because they had the highest biochar dosage; the PBBR2.5 % samples exhibited a slower increase. During the non-growing season, the differences among the sample groups diminished, with all cumulative flux curves exhibiting

Table 5
Review of previous studies on carbon sequestration system.

Study		Carbon sequestration rate (kg CO_2 eq/m^2/yr)	Notes and explanations
Fan et al. (2020)		23.72–46.93	Waste materials were incorporated into LID facilities, and the resulting changes in SOC and plant-based carbon sequestration were measured. The carbon sequestration rate of the LID facilities was determined to be 6.47–12.8 kg C/m^2/yr, which corresponds to 23.72–46.93 kg CO_2 eq/m^2/yr according to standard conversion factors.
Seyedabadi et al. (2021)		25.66–34.06	The carbon sequestered by aboveground vegetation within LID facilities was quantified, and the reduction in energy consumption caused by these facilities was determined. On the basis of these results, the maximum carbon sequestration was estimated to be 6.999–9.29 kg C/m^2/yr, which corresponds to 25.663–34.06 kg CO_2 eq/m^2/yr.
Kavehei et al. (2019)		~1.14	The soil carbon sequestration in 25 LID facilities was assessed using an elemental analyzer. The average sequestration rate of these facilities was determined to be 0.31 kg C/m^2/yr, which is equivalent to approximately 1.14 kg CO_2eq/m^2/yr. These values are notably lower than that observed in the present study, likely because of differences in measurement methodologies and site-specific climatic conditions.
Robbiati et al. (2023)		70.83	By quantifying plant biomass (both aboveground and belowground) and SOC within LID facilities, Robbiati et al. (2023) determined that a single growing season can result in the sequestration of up to 2.74 kg CO_2 eq/m^2. Moreover, they estimated the reductions in energy consumption caused by LID facilities, finding that these facilities can reduce annual CO_2 emissions by approximately 70.83 kg CO_2 eq/m^2/yr.
This study	Bioretention system with 10 % peat (PBR)	28.26	Annual carbon sequestration data were obtained through direct measurements conducted under conditions without biochar amendment.
	Peat-based bioretention system with 2.5 % biochar (PBBR2.5 %)	30.06	The addition of 2.5 % biochar to the PBR system resulted in a modest increase in the annual carbon sequestration rate.
	Peat-based bioretention with system 5 % biochar (PBBR5%)	36.65	The addition of 5 % biochar to the PBR system resulted in the highest annual carbon sequestration rate while simultaneously improving water quality and hydrological performance.
	Peat-based bioretention system with 10 % biochar (PBBR10%)	36.22	The addition of 10 % biochar to the PBR system, resulted in a slightly lower annual carbon sequestration rate than that achieved under the addition of 5 % biochar to this system. The results indicate that excess biochar application can reduce sequestration performance and adversely affect certain water quality parameters.

LID: low-impact development; SOC: soil organic carbon.

flat trends. These results indicate that the carbon sequestration benefits of biochar are most pronounced under favorable environmental conditions. Furthermore, biochar not only influenced carbon flux but also modified the soil environment. It improved water retention and soil structure, resulting in the biochar-enhanced soils retaining more moisture during dry periods, thus supporting sustained plant CO_2uptake. These soils also exhibited improved drainage during intense rainfall, which reduced waterlogging and ensured the maintenance of root respiration. Thus, the biochar-amended soils demonstrated greater resilience to climatic variability than did the PBR system, maintaining more stable carbon sequestration performance under fluctuating environmental conditions.

In addition to gas flux monitoring, Phase II involved bimonthly sampling for assessing changes in SOC. Baseline SOC values measured before this experiment were used to track temporal variations in SOC (Fig. 10). The SOC content of the PBR samples exhibited a continuous decline from 22.3 to 18.1 g/kg (a reduction of 4.2 g/kg), likely because of rapid root establishment and nutrient absorption in the newly planted system (Kumar et al., 2021). The decline later stabilized, potentially because of the depletion of easily decomposable carbon. By contrast, the biochar-containing samples initially exhibited an increase in SOC content with time. The SOC contents of the PBBR2.5 %, PBBR5%, and PBBR10 % samples increased from 22.3 to 24.0 g/kg (an increase of 1.7 g/kg), from 23.7 to 25.1 g/kg (an increase of 1.4 g/kg), and from 25.0 to 25.6 g/kg (an increase of 0.6 g/kg), respectively. This indicates that biochar promotes early carbon accumulation, following which the carbon level stabilizes. Overall, the biochar-containing systems exhibited stable or slightly increasing SOC levels with time, whereas the control PBR system exhibited a continuous decline in SOC with time.

Biochar also plays a key role in modulating microbial communities and carbon cycling, often slowing the mineralization of existing SOC (Kalu et al., 2024). A negative priming effect was observed in this

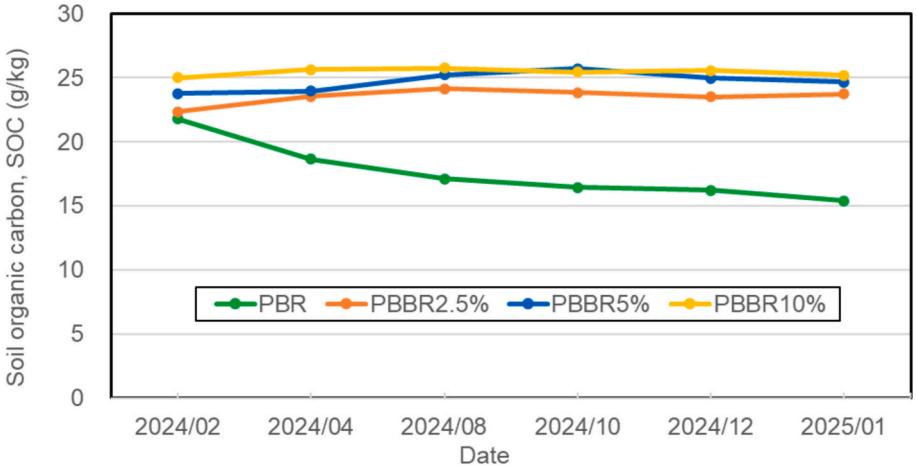

Fig. 10. Variations in the SOC contents of different bioretention samples over time.

study's experiment, where biochar suppressed the breakdown of native and newly added organic matter, thus reducing carbon loss in the form of CO_2. It also enhanced microbial biomass carbon and carbon use efficiency, or the proportion of assimilated carbon retained in microbial biomass rather than lost as respiration. Consequently, more carbon was converted into stable microbial residues.

In summary, biochar contributes stable carbon, decelerates carbon degradation, and inhibits microbial decomposition because of its aromatic-rich structure, which is formed through pyrolysis. This recalcitrance ensures long-term carbon retention in soil. Furthermore, biochar may produce physical barriers or microsites that protect organic matter from microbial breakdown (Gross et al., 2024). These factors may explain the sustained or increasing SOC trends with time in the biochar-containing samples of this study.

A biochar level of 5 % optimizes the generation of stable carbon and microbial carbon conversion, which maximizes overall SOC accumulation. Excessive biochar levels (e.g., PBBR10%) may inhibit microbial activity despite biochar contributing inert carbon. In this study, the PBBR10 % samples had high initial SOC content, with this exhibiting minimal changes over time, indicative of passive carbon retention. By contrast, the PBBR5 % samples achieved comparable final SOC values to those of the PBBR10 % samples through the synergistic effects of stable carbon input and active microbial utilization.

3.5. Comprehensive performance evaluation of different bioretention systems

This study evaluated the hydrological regulation, water quality improvement, and carbon sequestration performance of the PBR, PBBR2.5 %, PBBR5%, and PBBR10 % samples. Eight performance indicators were selected for a comprehensive assessment: saturated hydraulic conductivity (K_{sat}), WHC, NH_4–N removal rate, NO_3–N removal rate, PO_4^{3-} removal rate, COD removal rate, CO_2 sequestration flux, and SOC. These indicators collectively reflect the multifaceted effects of biochar amendment on the functionality of bioretention systems. The performance evaluation results are summarized in Table 6.

As illustrated in Fig. 11, the addition of biochar to the bioretention media did not universally enhance all performance metrics. The NH_4–N and PO_4^{3-} removal rates of the four types of samples did not exhibit significant differences, suggesting that the presence and dosage of biochar had limited effects on these two water quality parameters. By contrast, the other indicators exhibited notable improvements following biochar addition, with the most pronounced enhancements observed in K_{sat}, CO_2 sequestration flux, and SOC. However, when the biochar content was increased to 10 %, the NO_3–N and COD removal rates decreased to levels below those of the control PBR samples. This finding indicates that excessive biochar amendment can suppress certain purification mechanisms, potentially undermining the treatment capacity for specific pollutants.

Table 6
Performance evaluation results for the four examined bioretention systems.

Indicator	Bioretention mesocosms			
	PBR	PBBR2.5 %	PBBR5%	PBBR10%
Ksat (cm/s)	0.0392 ± 0.0077	0.0493 ± 0.0013	**0.0601 ± 0.0025**	0.0513 ± 0.0016
WHC (%)	49.5 ± 2.7	52.7 ± 1.9	53.1 ± 2.6	**54.2 ± 2.2**
NH_4-N removal (%)	87.92 ± 2.63	89.03 ± 1.41	89.46 ± 1.87	**90.95 ± 1.42**
NO_3^- removal (%)	63.05 ± 8.18	67.20 ± 5.01	**75.67 ± 3.79**	60.65 ± 6.58
PO_4^{3-} removal (%)	82.93 ± 1.98	84.54 ± 2.49	83.59 ± 1.94	**84.79 ± 1.86**
COD removal (%)	83.36 ± 3.08	**94.49 ± 1.12**	88.99 ± 1.73	59.07 ± 6.10
Carbon sequestration (kg CO_2 eq/m^2/mo)	2.36 ± 0.45	2.51 ± 0.51	**3.05 ± 0.59**	3.02 ± 0.64
SOC (g/kg)	22.3 to 18.1 (−4.2)	**22.3 to 24.0 (+1.7)**	23.7 to 25.1 (+1.4)	25.0 to 25.6 (+0.6)

Note: bold values indicate the best performance for each indicator.

Overall, the comprehensive performance evaluation indicated that the PBBR5 % samples provided the most balanced and effective improvements across all adapted metrics. These samples had the highest K_{sat} values and NO_3–N removal rates. They also exhibited the second-best results (after the PBBR10 % samples) on most other metrics. Thus, the addition of 5 % biochar to PBR systems achieves an optimal balance between performance enhancement and system stability. The PBBR2.5 % samples also exhibited noticeable improvements in the evaluation metrics compared with the PBR samples. Therefore, PBBR2.5 % systems can serve as viable alternatives to PBBR5 % systems, especially under conditions in which low biochar usage is preferred. The PBBR10 % samples exhibited excellent results in terms of the NH_4-N removal rate, WHC, CO_2 sequestration flux, and SOC content; however, they had a low COD removal efficiency, indicating that caution should be exercised in their application. The potential trade-offs associated with excessive amendment highlight the importance of optimizing biochar dosage for maximizing performance of bioretention systems.

4. Conclusion and recommendations

This study examined the effects of biochar content on the performance of bioretention cells, and found that appropriate quantities of biochar can significantly enhance the performance of bioretention systems in terms of hydrological regulation, pollutant removal, and carbon sequestration. A biochar content of 5 % offered the most balanced improvement, enhancing saturated hydraulic conductivity and WHC without compromising infiltration efficiency. Biochar contents of 2.5 % and 5 % improved soil structure and water retention. By contrast, a 10 % biochar content disrupted macropore connectivity, reduced the NO_3–N removal efficiency, and increased effluent COD concentrations due to pH changes and DOC leaching.

Biochar's porous structure and surface chemistry facilitated the adsorption of nutrients and organic pollutants, increasing the hydraulic retention time and supporting microbial processes such as nitrification–denitrification and organic matter degradation. Moreover, a positive correlation was observed between biochar dosage and CO_2 sequestration capacity up to a biochar dosage of 5 %. The average annual carbon sequestration of the control PBR group (no biochar) was 28.26 kg CO_2 eq/m^2/yr, and those of PBR groups with 2.5 %, 5 %, and 10 % biochar were 30.06, 36.65, and 36.22 kg CO_2 eq/m^2/yr, respectively. These results indicate that a biochar content of 5 % can substantially enhance carbon sink functions, offering a viable strategy for greenhouse gas mitigation. However, a further increase in biochar content can reduce CO_2 sequestration. All carbon flux calculations in this study reflect only the post-amendment phase. Emissions associated with biochar production were not included.

Overall, biochar exhibits high potential for integration into LID systems, offering synergistic benefits for runoff control, pollutant removal, and greenhouse gas reduction. However, the biochar content must be carefully calibrated according to site-specific objectives to balance ecological function and long-term sustainability. Due to experimental and equipment constraints, only one mesocosm was assigned to each treatment in this study. Each mesocosm was monitored over a period of 6 to 12 months. Temporal variability was considered in monthly standard deviations, yet natural and operational fluctuations remain a limitation. Future studies are encouraged to employ multiple replicates and extended monitoring durations to improve the statistical robustness and temporal resolution of key performance metrics such as CO_2 fluxes and pollutant removal efficiencies. In this study, microbial processes were likely responsible for the nutrient removal, COD degradation, and carbon cycling effects of biochar. Microbial processes were

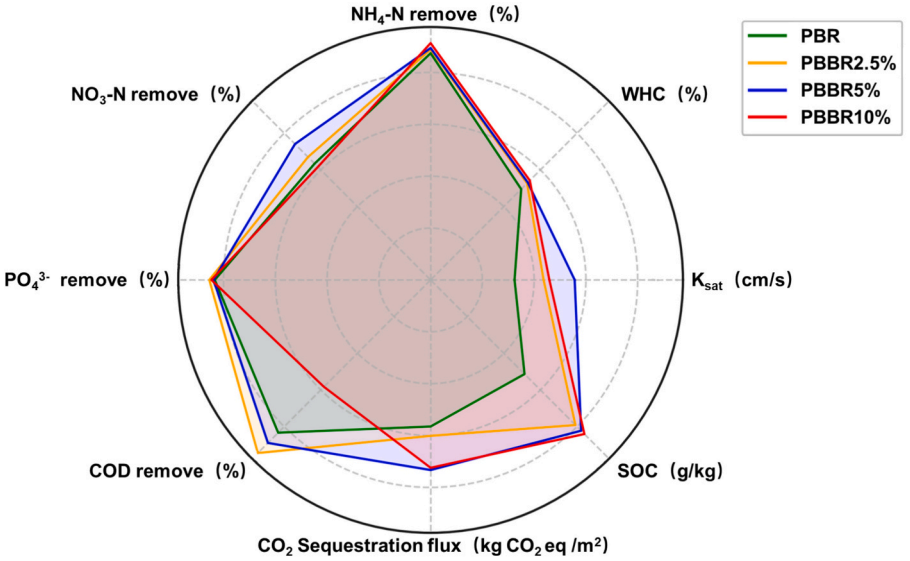

Fig. 11. Comprehensive performance of bioretention systems with varying biochar contents.

inferred based on literature and indirect indicators; no direct microbiological measurements were conducted. However, this interpretation is speculative due to the lack of direct microbial data, which represents a limitation of the current study. Therefore, future research should employ molecular biological techniques and enzyme assays to assess the responses of microbial communities under different biochar amendment rates and quantify their contributions to pollutant removal and carbon stabilization. Researchers can also systematically investigate the adsorption stability of biochar under variable operational conditions, the risk of pollutant rerelease, and strategies for mitigating such risks (e.g., appropriate media selection or operational optimization). In addition, long-term field monitoring is required to evaluate the temporal dynamics of biochar–microbe interactions, the stability of bioretention systems, and practical considerations such as economic feasibility and maintenance. Future studies should conduct comprehensive assessments of greenhouse gas emissions, including methane and nitrous oxide emissions, to characterize in detail the net climate impact of biochar-amended bioretention systems. Finally, researchers should develop comprehensive integrated models that can predict the socioeconomic, environmental, and hydrological benefits of bioretention cells under different rainfall and urban development patterns.

CRediT authorship contribution statement

Chia-Chun Ho: Writing – review & editing, Writing – original draft, Project administration, Methodology, Formal analysis, Conceptualization. **Yu-Qian Su:** Writing – original draft, Visualization, Investigation, Data curation. **Pen-Chi Chiang:** Supervision, Project administration, Funding acquisition.

Funding sources

This study was funded by the National Science and Technology Council of Taiwan and the Dr. Jentai Yang Sustainable Environmental Protection and Eco-humanistic Education Fund which is administered by the Overseas Chinese Environmental Engineers and Scientists Association.

Declaration of competing interest

The authors declare the following financial interests/personal relationships which may be considered as potential competing interests:

Pen-Chi Chiang reports financial support was provided by National Science and Technology Council, Taiwan. Chia-Chun Ho reports administrative support was provided by Dr. Jentai Yang Sustainable Environmental Protection and Eco-humanistic Education Fund. If there are other authors, they declare that they have no known competing financial interests or personal relationships that could have appeared to influence the work reported in this paper.

Data availability

No data was used for the research described in the article.

References

Ahmad Bhat, S., Kuriqi, A., Dar, M.U.D., Bhat, O., Sammen, S.S., Towfiqul Islam, A.R.M., et al., 2022. Application of biochar for improving physical, chemical, and hydrological soil properties: a systematic review. Sustainability 14, 11104.

Akpinar, D., Tian, J., Shepherd, E., Imhoff, P.T., 2023. Impact of wood-derived biochar on the hydrologic performance of bioretention media: effects on aggregation, root growth, and water retention. J. Environ. Manage. 339, 117864.

Alghamdi, A.G., Alkhasha, A., Ibrahim, H.M., 2020. Effect of biochar particle size on water retention and availability in a sandy loam soil. J. Saudi Chem. Soc. 24, 1042–1050.

Batalini de Macedo, M., Nóbrega Gomes Júnior, M., Pereira de Oliveira, T.R., H. Giacomoni, M., Imani, M., Zhang, K., et al., 2022. Low impact development practices in the context of United Nations Sustainable Development Goals: a new concept, lessons learned and challenges. Crit. Rev. Environ. Sci. Technol. 52, 2538–2581.

Batista, E.M., Shultz, J., Matos, T.T., Fornari, M.R., Ferreira, T.M., Szpoganicz, B., et al., 2018. Effect of surface and porosity of biochar on water holding capacity aiming indirectly at preservation of the Amazon biome. Sci. Rep. 8, 10677.

Bikbulatova, S., Tahmasebi, A., Zhang, Z., Rish, S.K., Yu, J., 2018. Understanding water retention behavior and mechanism in bio-char. Fuel Process. Technol. 169, 101–111.

Björklund, K., Li, L., 2017. Removal of organic contaminants in bioretention medium amended with activated carbon from sewage sludge. Environ. Sci. Pollut. Res. 24, 19167–19180.

Celik, I., Gunal, H., Budak, M., Akpinar, C., 2010. Effects of long-term organic and mineral fertilizers on bulk density and penetration resistance in semi-arid Mediterranean soil conditions. Geoderma 160, 236–243.

Dai, Y., Wang, W., Lu, L., Yan, L., Yu, D., 2020. Utilization of biochar for the removal of nitrogen and phosphorus. J. Clean. Prod. 257, 120573.

Davis, A.P., 2008. Field performance of bioretention: hydrology impacts. J. Hydrol. Eng. 13, 90–95.

Davis, A.P., Hunt, W.F., Traver, R.G., Clar, M., 2009. Bioretention technology: overview of current practice and future needs. J. Environ. Eng. 135, 109–117.

de Jesus Duarte, S., Glaser, B., Pellegrino Cerri, C.E., 2019. Effect of biochar particle size on physical, hydrological and chemical properties of loamy and sandy tropical soils. Agronomy 9, 165.

Deng, S., Wei, H., Chen, T., Wang, B., Huang, J., Yu, G., 2014. Superior CO2 adsorption on pine nut shell-derived activated carbons and the effective micropores at different temperatures. Chem. Eng. J. 253, 46–54.

Fan, L., Wang, J., Liu, X., Luo, H., Zhang, K., Fu, X., et al., 2020. Whether the carbon emission from green roofs can be effectively mitigated by recycling waste building

material as green roof substrate during five-year operation? Environ. Sci. Pollut. Res. 27, 40893–40906.
Feng, L., Gao, Z., Hu, T., He, S., Liu, Y., Jiang, J., et al., 2023. Performance and mechanisms of biochar-based materials additive in constructed wetlands for enhancing wastewater treatment efficiency: a review. Chem. Eng. J. 471, 144772.
Gogoi, A., Ahirwal, J., Sahoo, U.K., 2021. Plant biodiversity and carbon sequestration potential of the planted forest in Brahmaputra flood plains. J. Environ. Manage. 280, 111671.
Goldschmidt, A., Buffam, I., 2023. Biochar-amended substrate improves nutrient retention in green roof plots. Nat. Based Solut. 3, 100066.
Granata, M.U., Bracco, F., Catoni, R., 2020. Carbon dioxide sequestration capability of hazelnut orchards: daily and seasonal trends. Energy Ecol. Environ. 5, 153–160.
Gross, A., Bromm, T., Polifka, S., Fischer, D., Glaser, B., 2024. Long-term biochar and soil organic carbon stability – evidence from field experiments in Germany. Sci. Total Environ. 954, 176340.
Günal, E., Erdem, H., Çelik, İ., 2018. Effects of three different biochars amendment on water retention of silty loam and loamy soils. Agric Water Manag 208, 232–244.
He, Y., Zhou, X., Jiang, L., Li, M., Du, Z., Zhou, G., et al., 2017. Effects of biochar application on soil greenhouse gas fluxes: a meta-analysis. GCB Bioenergy 9, 743–755.
He, W., Lin, X., Shi, Z., Yu, J., Ke, S., Lu, X., et al., 2022. Nutrient removal performance and microbial community analysis of amended bioretention column for rainwater runoff treatment. J. Clean. Prod. 374, 133974.
Hobbie, S.E., Eddy, W.C., Buyarski, C.R., Adair, E.C., Ogdahl, M.L., Weisenhorn, P., 2012. Response of decomposing litter and its microbial community to multiple forms of nitrogen enrichment. Ecological monographs 82, 389–405.
Irfan, M., Hussain, Q., Khan, K.S., Akmal, M., Ijaz, S.S., Hayat, R., et al., 2019. Response of soil microbial biomass and enzymatic activity to biochar amendment in the organic carbon deficient arid soil: a 2-year field study. Arab. J. Geosci. 12, 1–9.
Jačka, L., Trakal, L., Ouředníček, P., Pohořelý, M., Šípek, V., 2018. Biochar presence in soil significantly decreased saturated hydraulic conductivity due to swelling. Soil Tillage Res. 184, 181–185.
Ji, C., Jin, Y., Li, C., Chen, J., Kong, D., Yu, K., et al., 2018. Variation in soil methane release or uptake responses to biochar amendment: a separate meta-analysis. Ecosystems 21, 1692–1705.
Ji, Y., Zhang, C., Zhang, X., Xie, P., Wu, C., Jiang, L., 2022. A high adsorption capacity bamboo biochar for CO2 capture for low temperature heat utilization. Sep. Purif. Technol. 293, 121131.
Kalu, S., Seppänen, A., Mganga, K.Z., Sietiö, O.-M., Glaser, B., Karhu, K., 2024. Biochar reduced the mineralization of native and added soil organic carbon: evidence of negative priming and enhanced microbial carbon use efficiency. Biochar 6, 7.
Kang, Y., Ma, H., Jing, Z., Zhu, C., Li, Y., Wu, H., et al., 2023. Enhanced benzofluoranthrene removal in constructed wetlands with iron-modified biochar: mediated by dissolved organic matter and microbial response. J. Hazard. Mater. 443, 130322.
Kavehei, E., Jenkins, G., Adame, M., Lemckert, C., 2018. Carbon sequestration potential for mitigating the carbon footprint of green stormwater infrastructure. Renew. Sustain. Energy Rev. 94, 1179–1191.
Kavehei, E., Jenkins, G.A., Lemckert, C., Adame, M.F., 2019. Carbon stocks and sequestration of stormwater bioretention/biofiltration basins. Ecol. Eng. 138, 227–236.
Kazemi, F., Beecham, S., Gibbs, J., 2011. Streetscape biodiversity and the role of bioretention swales in an Australian urban environment. Landsc. Urban Plan. 101, 139–148.
Kim, D., Park, T., Hyun, K., Lee, W., 2013. Life cycle greenhouse-gas emissions from urban area with low impact development (LID). Adv. Environ. Res. 2, 279–290.
Kinney, T., Masiello, C., Dugan, B., Hockaday, W., Dean, M., Zygourakis, K., et al., 2012. Hydrologic properties of biochars produced at different temperatures. Biomass Bioenergy 41, 34–43.
Kratky, H., Li, Z., Yu, T., Li, X., Jia, H., 2021. Study on bioretention for stormwater management in cold climate, part II: water quality. J. Water Clim. Chang. 12, 3582–3601.
Kumar, A., Singh, E., Singh, L., Kumar, S., Kumar, R., 2021. Carbon material as a sustainable alternative towards boosting properties of urban soil and foster plant growth. Sci. Total Environ. 751, 141659.
Li, Z.-g., Gu, C.-m., Zhang, R.-h., Ibrahim, M., Zhang, G.-s., Wang, L., et al., 2017. The benefic effect induced by biochar on soil erosion and nutrient loss of slopping land under natural rainfall conditions in central China. Agric. Water Manag. 185, 145–150.
Li, Y., Wang, X., Niu, Y., Lian, J., Luo, Y., Chen, Y., et al., 2018. Spatial distribution of soil organic carbon in the ecologically fragile Horqin Grassland of northeastern China. Geoderma 325, 102–109.
Li, M., Zhang, Z., Li, Z., Wu, H., 2020. Removal of nitrogen and phosphorus pollutants from water by $FeCl_3$-impregnated biochar. Ecol. Eng. 149, 105792.
Li, L., Zhang, Y.-J., Novak, A., Yang, Y., Wang, J., 2021. Role of biochar in improving sandy soil water retention and resilience to drought. Water 13, 407.
Lim, T.J., Spokas, K.A., Feyereisen, G., Novak, J.M., 2016. Predicting the impact of biochar additions on soil hydraulic properties. Chemosphere 142, 136–144.
Liu, C.-H., Chu, W., Li, H., Boyd, S.A., Teppen, B.J., Mao, J., et al., 2019. Quantification and characterization of dissolved organic carbon from biochars. Geoderma 335, 161–169.
Liu, X., Wang, W., Peñuelas, J., Sardans, J., Chen, X., Fang, Y., et al., 2022. Effects of nitrogen-enriched biochar on subtropical paddy soil organic carbon pool dynamics. Sci. Total Environ. 851, 158322.
Lu, Y., Gu, K., Shen, Z., Tang, C.-S., Shi, B., Zhou, Q., 2023. Biochar implications for the engineering properties of soils: a review. Sci. Total Environ. 888, 164185.
Mao, X., Jia, H., Yu, S.L., 2017. Assessing the ecological benefits of aggregate LID-BMPs through modelling. Ecol. Model. 353, 139–149.
Mensah, A.K., Frimpong, K.A., 2018. Biochar and/or compost applications improve soil properties, growth, and yield of maize grown in acidic rainforest and coastal savannah soils in Ghana. Int. J. Agron. 2018, 6837404.
Mukherjee, A., Zimmerman, A.R., 2013. Organic carbon and nutrient release from a range of laboratory-produced biochars and biochar–soil mixtures. Geoderma 193, 122–130.
Muñoz, C., Ginebra, M., Zagal, E., 2019. Variation of greenhouse gases fluxes and soil properties with addition of biochar from farm-wastes in volcanic and non-volcanic soils. Sustainability 11, 1831.
Nair, S., George, B., Malano, H.M., Arora, M., Nawarathna, B., 2014. Water–energy–greenhouse gas nexus of urban water systems: review of concepts, state-of-art and methods. Resour. Conserv. Recycl. 89, 1–10.
Oertel, C., Matschullat, J., Zurba, K., Zimmermann, F., Erasmi, S., 2016. Greenhouse gas emissions from soils—a review. Geochemistry 76, 327–352.
Oldfield, T.L., Sikirica, N., Mondini, C., López, G., Kuikman, P.J., Holden, N.M., 2018. Biochar, compost and biochar-compost blend as options to recover nutrients and sequester carbon. J. Environ. Manage. 218, 465–476.
Quan, C., Zhou, Y., Wang, J., Wu, C., Gao, N., 2023. Biomass-based carbon materials for CO2 capture: a review. J. CO_2 Util. 68, 102373.
Rivers, E.N., Heitman, J.L., McLaughlin, R.A., Howard, A.M., 2021. Reducing roadside runoff: tillage and compost improve stormwater mitigation in urban soils. J. Environ. Manage. 280, 111732.
Robbiati, F.O., Natalia, C., Gustavo, B., Gustavo, O., Jim, C.Y., Mario, S., et al., 2023. Vegetated roofs as a nature-based solution to mitigate climate change in a semiarid city. Nat.-Based Solut. 3, 100069.
Roy-Poirier, A., Champagne, P., Filion, Y., 2010. Review of bioretention system research and design: past, present, and future. J. Environ. Eng. 136, 878–889.
Samaraweera, H., Palansooriya, K.N., Dissanayake, P.D., Khan, A.H., Sillanpää, M., Mlsna, T., 2023. Sustainable phosphate removal using Mg/Ca-modified biochar hybrids: current trends and future outlooks. Case Stud. Chem. Environ. Eng. 8, 100528.
Sánchez, A., Artola, A., Font, X., Gea, T., Barrena, R., Gabriel, D., et al., 2015. Greenhouse gas emissions from organic waste composting. Environ. Chem. Lett. 13, 223–238.
Sanchez-Monedero, M., Cayuela, M.L., Roig, A., Jindo, K., Mondini, C., Bolan, N., 2018. Role of biochar as an additive in organic waste composting. Bioresour. Technol. 247, 1155–1164.
Sayara, T., Basheer-Salimia, R., Hawamde, F., Sánchez, A., 2020. Recycling of organic wastes through composting: process performance and compost application in agriculture. Agronomy 10, 1838.
Serafin, J., Narkiewicz, U., Morawski, A.W., Wróbel, R.J., Michalkiewicz, B., 2017. Highly microporous activated carbons from biomass for CO2 capture and effective micropores at different conditions. J. CO_2 Util. 18, 73–79.
Seyedabadi, M.R., Eicker, U., Karimi, S., 2021. Plant selection for green roofs and their impact on carbon sequestration and the building carbon footprint. Environ. Chall. 4, 100119.
Shamrikova, E., Kondratenok, B., Tumanova, E., Vanchikova, E., Lapteva, E., Zonova, T., et al., 2022. Transferability between soil organic matter measurement methods for database harmonization. Geoderma 412, 115547.
Sheng, Y., Zhu, L., 2018. Biochar alters microbial community and carbon sequestration potential across different soil pH. Sci. Total Environ. 622–623, 1391–1399.
Singh, E., Mishra, R., Kumar, A., Shukla, S.K., Lo, S.-L., Kumar, S., 2022. Circular economy-based environmental management using biochar: driving towards sustainability. Process Saf. Environ. Prot. 163, 585–600.
Steiner, C., Teixeira, W.G., Lehmann, J., Nehls, T., de Macêdo, J.L.V., Blum, W.E., et al., 2007. Long term effects of manure, charcoal and mineral fertilization on crop production and fertility on a highly weathered Central Amazonian upland soil. Plant Soil 291, 275–290.
Tian, J., Jin, J., Chiu, P.C., Cha, D.K., Guo, M., Imhoff, P.T., 2019. A pilot-scale, bi-layer bioretention system with biochar and zero-valent iron for enhanced nitrate removal from stormwater. Water Res. 148, 378–387.
Tsai, C.-C., Chang, Y.-F., 2021. Quality evaluation of poultry litter biochar produced at different pyrolysis temperatures as a sustainable management approach and its impact on soil carbon mineralization. Agronomy 11, 1692.
Ulrich, B.A., Loehnert, M., Higgins, C.P., 2017. Improved contaminant removal in vegetated stormwater biofilters amended with biochar. Environ. Sci.: Water Res. Technol. 3, 726–734.
Vassilev, S.V., Baxter, D., Andersen, L.K., Vassileva, C.G., 2010. An overview of the chemical composition of biomass. Fuel 89, 913–933.
Wu, W., Wu, C., Zhang, G., Liu, J., Li, Y., Li, G., 2023. Synthesis and characterization of magnetic K2CO3-activated carbon produced from bamboo shoot for the adsorption of rhodamine b and CO2 capture. Fuel 332, 126107.
Xiong, J., Liang, L., Shi, W., Li, Z., Zhang, Z., Li, X., et al., 2022. Application of biochar in modification of fillers in bioretention cells: a review. Ecol. Eng. 181, 106689.
Xu, H.-J., Wang, X.-H., Li, H., Yao, H.-Y., Su, J.-Q., Zhu, Y.-G., 2014. Biochar impacts soil microbial community composition and nitrogen cycling in an acidic soil planted with rape. Environ. Sci. Technol. 48, 9391–9399.
Xu, L., Fang, H., Deng, X., Ying, J., Lv, W., Shi, Y., et al., 2020. Biochar application increased ecosystem carbon sequestration capacity in a Moso bamboo forest. For. Ecol. Manage. 475, 118447.
Yang, C., Lu, S., 2021. Effects of five different biochars on aggregation, water retention and mechanical properties of paddy soil: a field experiment of three-season crops. Soil Tillage Res. 205, 104798.

Yu, X., Wu, C., Fu, Y., Brookes, P., Lu, S., 2016. Three-dimensional pore structure and carbon distribution of macroaggregates in biochar-amended soil. Eur. J. Soil Sci. 67, 109–120.
Zhao, J., Ren, T., Zhang, Q., Du, Z., Wang, Y., 2016. Effects of biochar amendment on soil thermal properties in the North China Plain. Soil Sci. Soc. Am. J. 80, 1157–1166.
Zhuang, L.-L., Li, M., Li, Y., Zhang, L., Xu, X., Wu, H., et al., 2022. The performance and mechanism of biochar-enhanced constructed wetland for wastewater treatment. J. Water Process Eng. 45, 102522.